Tunable Nanopatterning of Conductive Polymers via Electrohydrodynamic Lithography

Rickard, Jonathan James Stanley; Farrer, Ian; Goldberg Oppenheimer, Pola

DOI:
10.1021/acsnano.6b01246

Document Version
Publisher's PDF, also known as Version of record

Citation for published version (Harvard):
Rickard, JJS, Farrer, I & Goldberg Oppenheimer, P 2016, 'Tunable Nanopatterning of Conductive Polymers via Electrohydrodynamic Lithography', *ACS Nano*, vol. 10, no. 3, pp. 3865-3870.
https://doi.org/10.1021/acsnano.6b01246

ACS NANO

www.acsnano.org

ARTICLE

Tunable Nanopatterning of Conductive Polymers *via* Electrohydrodynamic Lithography

Jonathan James Stanley Rickard,[†,‡] Ian Farrer,[‡] and Pola Goldberg Oppenheimer*[,†]

[†]School of Chemical Engineering, University of Birmingham, Birmingham B15 2TT, United Kingdom

[‡]Department of Physics, Cavendish Laboratory, University of Cambridge, Cambridge CB3 0HE, United Kingdom

ABSTRACT: **An increasing number of technologies require the fabrication of conductive structures on a broad range of scales and over large areas. Here, we introduce advanced yet simple electrohydrodynamic lithography (EHL) for patterning conductive polymers directly on a substrate with high fidelity. We illustrate the generality of this robust, low-cost method by structuring thin polypyrrole films *via* electric-field-induced instabilities, yielding well-defined conductive structures with feature sizes ranging from tens of micrometers to hundreds of nanometers. Exploitation of a conductive polymer induces free charge suppression of the field in the polymer film, paving the way for accessing scale sizes in the low submicron range. We show the feasibility of the polypyrrole-based structures for field-effect transistor devices. Controlled EHL pattering of conductive polymer structures at the micro and nano scale demonstrated in this study combined with the possibility of effectively tuning the dimensions of the tailor-made architectures might herald a route toward various submicron device applications in supercapacitors, photovoltaics, sensors, and electronic displays.**

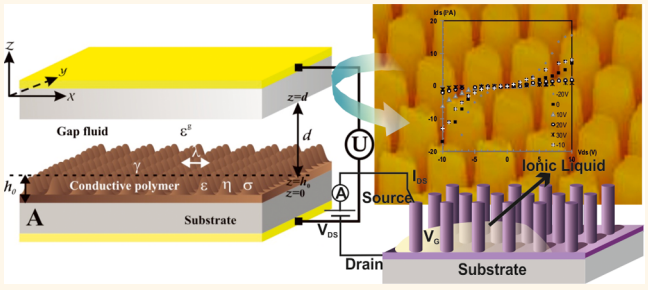

KEYWORDS: *conductive polymers, electrohydrodynamic lithography, leaky dielectrics, field-effect transistors*

Conductive polymers (CPs) combine properties of polymers with the electrical, chemical, and optical properties of metals. Straightforward processing, tunable optoelectronic properties *via* molecular design, high surface area, and the possibility of modifying conductivity by doping, are only a few of the advantages attributed to CPs. Considerable research has been directed toward studying CPs aiming for their potential implementation into a variety of functional devices, including field effect transistors (FETs),[1,2] organic light emitting diodes (OLEDs), integrated circuits, chemical and biological sensors,[3] and electrochromic devices.[4]

In order to take full advantage of the functions of π-conjugated macromolecules and, in particular, for generation of flexible organic electronics, patterning of CPs into structures ranging from 100 μm to sub-100 nm is required. Moreover, generation of high-fidelity submicrometer architectures with a good adhesion to the substrate in a controlled manner is essential to realize the full potential of CPs patterning for their future integration into applied devices.[5] Conducting polymer micro- and nanostructures can, for instance, be used for red, green, or blue (RGB) pixels in multicolour OLED displays and interconnects in all-polymer integrated circuits.[6]

Routes for patterning CPs have been explored extensively, and the most prominent techniques are soft-lithography,[7] electron beam lithography,[8] photochemical patterning by photolithography,[9,10] and nanoimprinting.[11] Hitherto, however, most of the existing approaches to pattern CPs exhibit limitations in certain aspects including resolution, position control, versatility, and reproducibility. Although some conventional lithographic techniques approach their physical limits, others are incompatible with CPs due to the poor adhesion between the polymers and the substrate. In light of the complexity involved in obtaining high resolution registration from soft-lithography, together with an increasing need to develop low-cost and high-throughput methods for patterning conductive polymer films, interest in alternative patterning processes has grown.

In the present work, we introduce an elegant, straightforward EHL technique for direct patterning of conductive polymers. Theoretical studies addressing pattern generation have predicted electrohydrodynamic pattern formation in conducting liquids;[12−14] yet, these have not been demonstrated to date. Herein, a versatile organic semiconductor, polypyrrole (PPy) film is patterned *via* the EHL technique enabling highly ordered structures which can be easily assembled into functional

Received: February 18, 2016
Accepted: February 23, 2016
Published: February 23, 2016

DOI: 10.1021/acsnano.6b01246
ACS Nano 2016, 10, 3865−3870

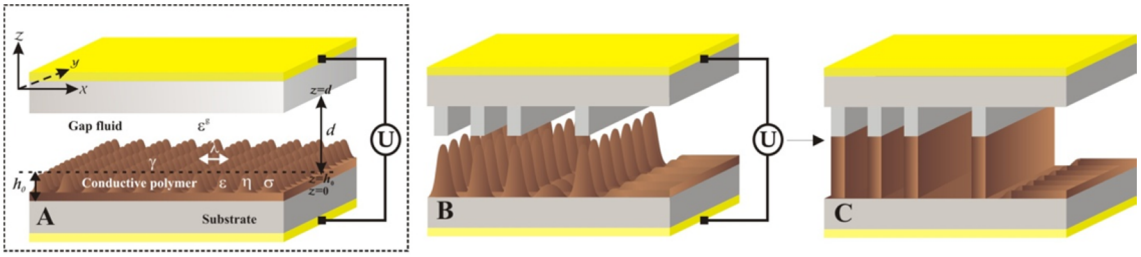

Figure 1. Schematic representation of electrically driven patterning setup. (A) Thin liquefied confined film develops characteristic undulations at $z = h_0$ while a constant voltage, U is applied to between the electrodes (or across the capacitor gap). Contact potentials at each interface give rise to the electric field, E_f that drives the flow. The dielectric constants of the film, ε and the gap ε^g mediate the electrical forces from the applied voltage. The electrostatic force is balanced by surface tension, γ yielding the characteristic spacing, λ of the instability with viscosity η. (B) Heterogeneous force field directs the instability toward the protruding line structures and generates columnar-bridges between the two electrodes, followed by a coarsening of the pillars yielding in a positive replica of the master pattern in (C). In unstructured regions, the film remains stable on a much longer time scale.

devices. This method provides a single-step and cost-effective approach for direct patterning of conjugated polymers on solid substrates, generating a variety of feature sizes ranging from tens of micrometers to hundreds of nanometers.[15−17] The EHL concept exploits an instability induced by an applied electric field across the liquefied polymer−air bilayer sandwiched between two-electrodes in a capacitor-like device. In the case of dielectric polymers, the electric field causes the energetically unfavorable buildup of displacement charges at the dielectric interface, leading to the alignment of the *dielectric* interface parallel to the electric field lines, which lowers the electrostatic energy. In a homogeneous electric field, this typically results in pillar structures that span the two electrodes. Because the total potential difference generated by the dipole layers at the interface is suppressed across the conductive liquid layer, the driving force of the pattern formation in the case of a *leaky dielectric* polymer subjected to the EHL patterning lies in the electric field in the air gap, E^1.[14] A subambient pressure within the film balances the electrostatic force due to the field in the air gap on the polymer−air interface, placing the film in tension, and therefore, generating the origin of the EHL instability. The intrinsic length scale of instabilities in thin films is on the order of microns. In order to exploit this natural structure formation process, it is important, first, to control the resulting pattern and, second, to decrease the length scale to technologically interesting feature sizes. Both requirements are fulfilled by imposing a laterally heterogeneous electric field with variations smaller than the intrinsic wavelength. Such a lateral field variation is typically achieved by using a topographically structured mask as one of the electrodes, thus enabling the generation of a broad variety of structures on different length scales. EHL can be used to fabricate patterns in a wide variety of polymers and composites using both featureless and topographically structured masks.[18] Patterning of thin films using electrohydrodynamic instabilities possesses many desired characteristics and has convincingly been used as a simple method to structure and replicate patterns of nonconducting, dielectric polymers (*e.g.*, polystyrene (PS), poly(methyl methacrylate), polycaprolactone, nanocomposite carbon nanotubes integrated in PS[18]) on *submicrometer* length scales targeting various applications. However, the applicability of this technique to a new range of materials, that is, conductive polymers, has not been demonstrated yet. Herein, EHL is shown to provide a low-cost, high-resolution patterning of functional π-conjugated polymers without compromising their properties and, therefore, enables a tunable method to fabricate and control the position and dimensions of the generated morphologies (by varying a number of experimental parameters, such as the initial film thickness, interelectrode spacing, applied voltage, surface tension, and lateral periodicity of the master electrode) at a low-cost, but this high-throughput technique also opens up a new avenue for patterning CPs targeting various applications including FETs, LEDs, solar-cells, advanced sensors and microelectronics.

RESULTS AND DISCUSSION

Owing to its high electroconductivity, good stability in ambient conditions, and facile processability, the intrinsically conducting PPy polymer has been a topic of extensive research concurrently focusing on practical applications and on synthesis. PPy can be synthesized by electrochemical or chemical polymerization methods. One of the main limiting factors has been its nonsolubility in any solvent due to the strong intermolecular interactions of the heterocyclic planar structure of PPy. Although electropolymerization yields predominantly rough films, which inhibits PPy electronic functions, whereas chemical polymerization results in insoluble powder. Because EHL lithography requires homogeneous films for the patterning process, an optimized synthesis of PPy[19] has been carried out in this study to prepare electroconductive PPy, which is soluble in organic solvents and can be spin-coated into uniform thin films. This process (described in the Methods Section) yielded 7% of pure PPy soluble in DMF, THF, *m*-cresol, and chloroform. The conductivity of the films was measured to be 1.7 ± 0.5 S/m (spin-cast from chloroform). The synthesized PPy was readily spin-cast into homogeneous films both on Si wafer substrates and on indium tin-oxide (ITO) glass, which serve as bottom electrodes during the patterning process. These conductive polymer films were then subjected to the EHL patterning process.

The physical mechanism of the EHL pattern formation process in the case of a perfect dielectric is well understood.[20,21] For EHL patterning of conductive polymers, however, free charges in the film (which substantially modify the electric field distribution in the film−air double layer) have to be taken into consideration. The following discussion is based on the formalism proposed by Pease and Russell[13,14] for charge-driven electrohydrodynamic patterning of leaky dielectric films.

The pattern selection of EHL instabilities is given in terms of a linear stability analysis for an incompressible Newtonian fluid assuming the nonslip boundary condition at the substrate

DOI: 10.1021/acsnano.6b01246
ACS Nano 2016, 10, 3865−3870

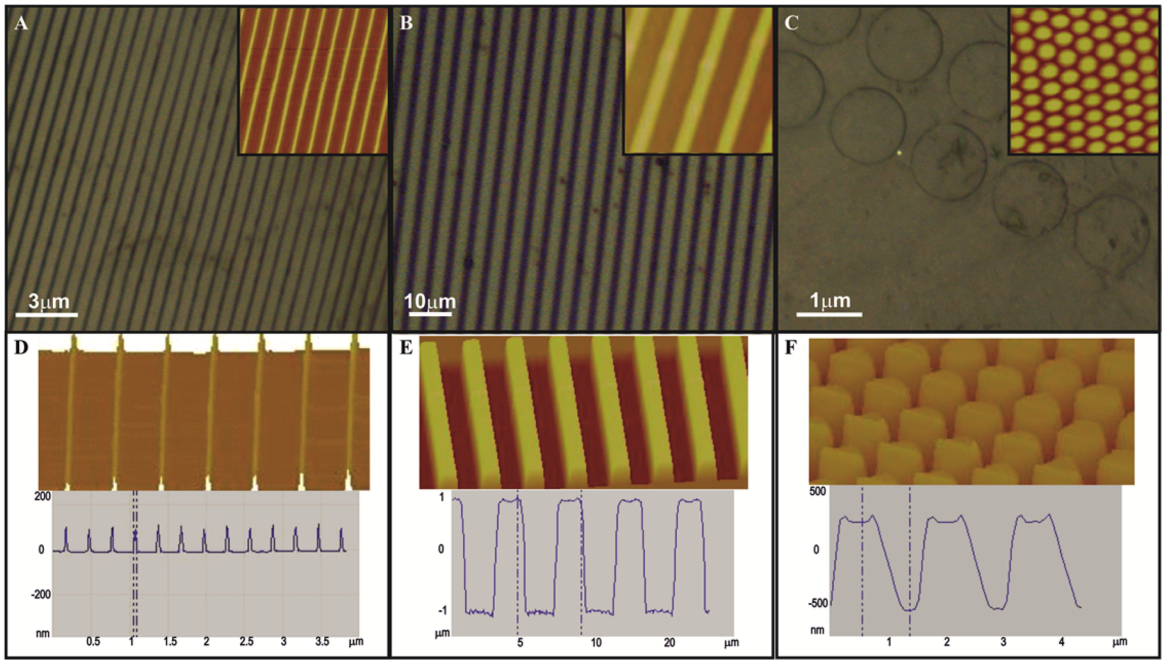

Figure 2. EHL replication of line and columnar patterns. Optical microscopy images with height AFM images (inset) and three-dimensional AFM micrographs with cross section analysis showing fabricated PPy structures: (A) and (D) 120 nm wide nanolines with a height of 100 nm; (C) and (F) submicrometer pillars with 700 nm in height, 1.2 μm in diameter and with a pitch of 0.5 and 2.5 μm wide and 2.0 μm height microlines (B) and (E).

(Figure 1A). The destabilizing electrostatic pressure, p scales with the square of an applied voltage, U

$$p = -\frac{1}{2}\frac{\varepsilon^g \varepsilon_0 U^2}{(d - h_0)^2} \tag{1}$$

with the capacitor electrode spacing, d, the dielectric permittivity of free space, ε_0, and the dielectric constant of the gap fluid, ε^g (which is an air gap in our case, *i.e.*, $\varepsilon^g = \varepsilon_1$). The conductivity of the leaky dielectric suppresses the electric field in the film and the field in the gap drives the EHL pattern formation. This yields the dimensionless conductivity, Σ representing the ratio of a time scale for free charge conduction to the process time scale

$$\sum = \frac{\sigma\eta\gamma(d - h_0)^3}{(\varepsilon_1)^3 \varepsilon_0^3 U^4} \tag{2}$$

where, γ is a surface tension, σ is a conductivity, and η is the viscosity of the polymer. With the limit of $\Sigma \gg 1$, (in our study E_f is on the order of 10^8) the most dominant (characteristic) wavelength

$$\lambda = \frac{(2\sqrt{2})\pi}{U}\sqrt{\frac{\gamma(d - h_0)^3}{\varepsilon_0}} \tag{3}$$

is given by a force balance between the destabilizing electrostatic pressure due to the field in the gap acting on the polymer–air interface with respect to the interfacial height, h_0 and the γ acting to minimize the surface area, thus suppressing the height variations. The characteristic time constant for the instability is given by

$$\tau = \frac{12\gamma\eta(d - h_0)^6}{U^4 h_0^3 \varepsilon_0^2} \tag{4}$$

The EHL patterning process of various structures is illustrated in Figure 1A–C. A topographically structured electrode induces an inhomogeneous electric field in the capacitor gap. Initial instabilities are coupled to the lateral field variation and further focused in the direction of the highest electrostatic force. They are thus driven toward the downward protruding structures of the top mask. This results in a pattern of pillars spanning the capacitor gap at the locations of the smallest interelectrode distances (Figure 1B), which by coalescence eventually generates a replicated pattern of the upper electrode (Figure 1C). The final height of the polymer structures is dictated by d and h_0. Despite the shorter destabilization time and faster growing modes of fully conducting material compared to a prefect dielectric (minutes *vs* hours[15,22]), smaller accessible scale-sizes (in the range of 100 nm (Figure 2A and D) *vs* the typical micrometer arrays[15,22,23]) and greater aspect ratios (*e.g.*, 0.83 in Figure 2), the pattern formation process of Figure 1 is reminiscent of the well-studied case of generic polymers,[20,21,24] thus confirming the same underlying physical mechanism. To note, EHL patterning has successfully taken place when using a heterogeneous electric field that is formed by using a structured rather than planar top electrode. Although for homogeneous E_f, patterning of CP was somewhat limited, by using topographically structured top electrode, it was possible to successfully modulate the electric field, decrease the characteristic wavelength and increase the aspect ratio of the structures without causing the electrical breakdown of the capacitor patterning device due to high external voltages. When a laterally varying electric field is applied to the capacitor device, the instability is focused in the direction of the highest electric field and because the electrostatic pressure is inversely proportional to a square of the capacitor gap, it is considerably stronger for smaller interelectrode distances.

DOI: 10.1021/acsnano.6b01246
ACS Nano 2016, 10, 3865–3870

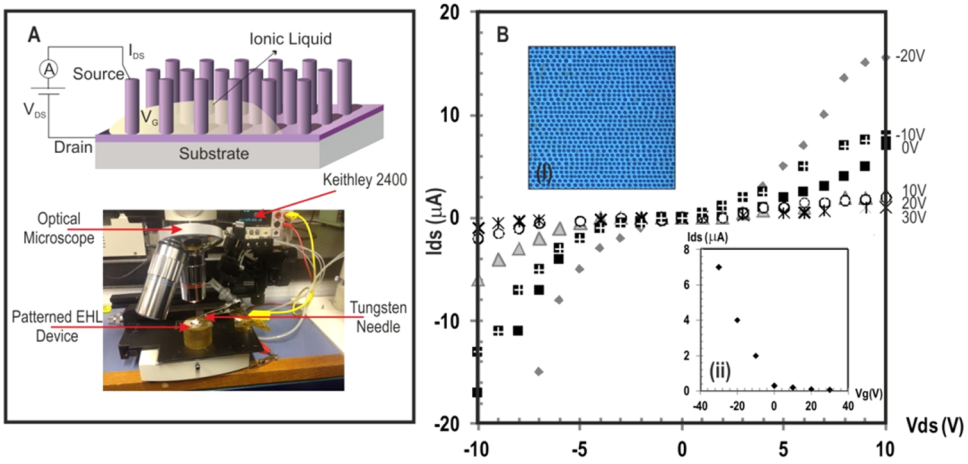

Figure 3. FET performance of EHL-PPy architectures. (A) Schematic representation (top) and an overview image (bottom) of the configuration of a liquid-ion gate vertical FET using the EHL-generated structures on top of Si-SiO_2 substrate. A probe tip comprised of a tungsten needle was employed under a 1000× magnification of an optical microscope to establish a good connection between the source and the drain. (B) Drain current *versus* drain voltage characteristics of PPY electrolyte-gated transistor based on EHL fabricated pillars shown in a top-view optical image (inset B,i) and gate voltage performance (inset B,ii) of the PPy-FET described in (A).

Figure 2 shows optical microscopy (top) and atomic force microscopy (AFM) (inset, height; bottom, three-dimensional) images of line and column patterns obtained after the application of a voltage to the capacitor device. Optical micrographs reveal large areas comprised of conductive PPy patterns exhibiting a range of feature sizes (Figure 2A–C). The cross-sectional AFM image in Figure 2B reveals a line height of 2.0 μm and a width of 2.5 μm. The length scale of the EHL formed patterns is dependent on the feature size of the structured electrode. A reduction in the topographically induced feature size and an increased electrical potential (75 V) results in PPy lines as small as 100 nm height and 120 nm width (Figure 2A). An additional pattern of ordered columns has been generated using EHL patterning after the application of 55 V between the electrodes. This has resulted in a columnar structure with a typical height of 700 nm, a diameter of 1.2 μm and a periodicity of 2 μm (Figure 2C). Apart from isolated defects, the patterns of the master electrodes were reproduced with high fidelity over the entire electrode area (typically 200 × 200 μm^2).

Dimensions of a semiconducting channel are known to have a direct impact on the device performance.[25,26] The final pattern morphology and its dimensions can be tuned by the specific set of sample parameters. The pattern formation rate, the height and the lateral dimensions (*i.e.*, structures width and spacing, and therefore, the aspect ratio) of the EHL generated patterns can be controlled *via* adjustment of the applied voltage (increasing U causes higher driving forces), the initial film thickness, the interelectrode gap, and the surface tension. Moreover, the imposed modulation periodicity of the structured electrode, for which the amplitude can be adapted, not only plays an important role in obtaining a faithful replication but also opens up a route toward decreasing the patterns length scale to the sub-100 nm range. In the presence of the laterally varying confinement, the liquid morphologies are organized according to the ratio of the plate spacing and the initial amount of polymer in the capacitor gap. Though the pattern selection during the early stage of the process is a sinusoidal surface undulation, for all samples, the filling ratio establishes the late stage of pattern formation. The final morphology of the replicated pattern is determined by the partial coalescence of the initial pattern.

The shape of the generated pattern depends on the ratio of the intrinsic film undulation wavelength and the lateral periodicity of the master electrode. Thus, sub-100 nm patterns with structure-to-structure spacing on the order of 100 nm can be achieved with a leaky dielectric by both exploiting conducting polymer as a film material and gap materials that combine a low interfacial tension with the film with a high electric strength.

Vertical FETs hold the potential to combine good performance with high device density. The application of vertical transistors in memory devices is especially sought after due to its potential in shrinking individual devices and capability of multilevel memory structures three-dimensionally. In order to evaluate the electrolyte-gated vertical FET performance, EHL-generated structure arrays were fabricated with gate length of 700 nm and a pitch of 500 nm as schematically shown in Figure 3A, top and 3B,i (top view optical microscopy image). Liquid-ion gate FET geometry was constructed using a potassium chloride (KCl) solution and tungsten needle as contacting electrode (Figure 3A). The electrical drain current (I_{DS})−drain voltage (V_{DS}) characteristics of the device as a function of different gate voltages (V_G) are shown in Figure 3B. Inset ii of Figure 3B, presents the transfer characteristics (source-drain current *versus* gate voltage, I_{DS}−V_G) at a constant drain-source voltage (a representative value of V_{DS} = 4 V). The positive gate voltages decrease the current and the values of I_{DS} increase upon raising the positive V_G at a negative V_{DS} indicating that the devices exhibit *p*-type FET behavior with the holes being the major charge carriers. This current modulation due to the modulation of carrier density in the PPy structures along with the onset of the saturation of drain-source voltage at approximately 9 V is consistent with the measurements previously performed on other PPy-based transistors[27,28] The maximum value of I_{SD} of the transistor was 20 mA in the 0.01 M KCl solution at V_G = 20 V.

Furthermore, structured conductive polymer based substrates exhibit an increased electrochemically accessible surface area along with the high electrical conductivity. They may be used to generate well-defined electrical contacts and may provide a

DOI: 10.1021/acsnano.6b01246
ACS Nano 2016, 10, 3865–3870

route for incorporating chemical functions by functionalization along their longtinudal axis. This is potentially useful for the development of rapid-response biochemical sensors, which are selective for targeted chemical and biological molecules. Additional optimization, currently underway, of the EHL generated electroconductive submicron structures will enable devices that can be used directly as arrays of electrodes to fabricate all plastic FETs and biochemical sensors. Along with promising electrical transistor characteristics, the use of low-cost lithographic technology and simple gate definition process steps could make such devices suitable candidates for next generation technology nodes.

CONCLUSIONS

In conclusion, a conducting polymer EHL patterning process is directly performed on silicon substrates yielding high fidelity structures with a range of feature scale sizes. Though patterning of PPy is a *proof-of-concept*, the versatile EHL patterning method can be applied to a variety of CPs. The feasibility of a PPy-EHL-based device as a FET is successfully demonstrated. With properly chosen experimental parameters, combined with a suitable master electrode, it should be possible to generate patterns with sub-100 nm widths over very large areas. Submicrometer structured conducting polymers possess improved properties and performance compared with bulk material devices. These structures have potential for applications in the development of microelectronics, displays, and biotechnological assemblies, such as flexible display devices or bio and chemical sensors. For example, high density electrically conducting microstructures can be directly used as miniaturized sensors. The EHL approach can be further extended to lateral complex or hierarchical structures consisting of bilayers or larger numbers of different materials with set mismatched conductivities.

This is the first time that a conductive polymer has been patterned using EHL technique. This method provides a promising route for a straightforward and cost-effective large area patterning of CPs, opening up many opportunities for high resolution and high throughput structures with applications in nano- and biotechnology related fields and devices.

METHODS

All the chemicals were purchased from Sigma-Aldrich and used without further purification. PPy soluble in organic solvents has been synthesized (with slight modifications) following the procedure described in ref 19: 0.14 g of dried pyrrole monomer was added to a solution comprised of 0.0745 mol of dodecylbenzenesulfonic acid (DBSA) dissolved in 300 mL of deionized water (DW) and dynamically stirred for 30 min. Then, 0.35 M of aqueous ammonium persulfate solution was added to this mixture and left to react for 18 h under continuous stirring. Addition of methanol stopped the reaction and the final solution was filtered to obtain black PPy powder. The PPy was washed several times with methanol and excess of DW followed by filtering, eventually yiding pure PPY. The molecular weight of PPy was 157 kg/mol and the glass transition temperature was 98 °C.

Highly polished *p*-doped silicon (Si) wafers, with ⟨100⟩ crystal orientation (Wafernet Gmbh, Eching, Germany) covered by 100 or 300 nm thick oxide layer were used as substrates. Patterned silicon wafers were obtained from X-lith eXtreme Lithography, Ulm, Germany). Chloroform (Fischer Inc.) was used as a main solvent.

Thin films were generated by spin-coating onto a silicon wafer substrate (dimensions of 1 × 1 cm^2) from chloroform solution with typical concentrations of 2−3% polymer by weight. Prior to spin-coating, the substrates were cleaned in a Piranha solution consisting of 3:1 H_2SO_4 (98%):H_2O_2 (30%), followed by thorough rinsing with deionized water and drying under nitrogen. To ensure the integrity of the formed structures, patterned electrodes were rendered hydrophobic by the deposition of a 1,1,1,2*H*-perfluorodecyltrichlorosilane self-assembled monolayer to reduce the adhesion between the mask and the polymer. Thereafter, substrates as well as electrodes covering the films were subjected to snow-jet cleaning immediately before film deposition and device assembply. Facing it, a topographically structured electrode was mounted at a specific distance using silicon oxide colloids as spacers, leaving a thin air gap, d (between the mask and the film, Figure 1A).

The spin-cast films were liquefied either by annealing above the softening temperature of the polymer or by exposing them to controlled chloroform vapor atmosphere to induce chain mobility and facilitate equilibration. The solvent vapor pressure was adjusted using a homemade apparatus. Mass-flow controllers (MKS Instruments Model 1179A with a PR4000F readout) regulated the flux of the carrier gas, N_2 through two lines. In one line, the N_2 was bubbled through a solvent-filled bottle resulting in a solvent-saturated gas stream. Both streams were mixed and passed through the sample chamber. The flow volumes per time were individually regulated to values between 1 and 20 cm^3 min^{-1}. The vapor pressure in the mixing chamber can be estimated by the ratio of the saturated (p_{sat}) to dry gas (p) flow as determined by the flow-meter readout. All tubes and connectors were made from solvent-resistant materials (glass and Teflon). The chamber and a regulated water bath containing the solvent bottle and the mixing chamber were held at the same temperature. Typical values for the vapor pressures were $p = p_{sat}$ = 0:5/0:7. The films were allowed to swell in the controlled solvent vapor atmosphere until they reached their equilibrium thickness after around 30 min. This condition was determined by experiments using a sample chamber lid with a window, providing optical access to the chamber. Using a light microscope in reflection mode the change in film thickness as a function of time was qualitatively monitored. A voltage of 45−80 V was then applied between the two electrodes. Cooling sample to RT, or removal of the solvent by passing dry nitrogen through the sample chamber, solidified the polymer before the voltage was removed, terminating the patterning process. After quenching the samples to room temperature, the electric field was disconnected and the upper electrode was removed.

The sample topography was analyzed by optical microscopy and atomic force microscopy. Olympus Optical Microscope GX61 was employed in our experiments. The reflection of white light from the sample enabled us to resolve submicrometer features. The acquired data in our experiments is complemented by the *in situ* monitoring of EHL pattern formation and replication in thin films, using a digital camera and imaging software (Carl Zeiss VisioCam). AFM measurements were performed using a Nanoscope IV Dimension 3100 (Veeco Instruments Inc.) microscope operated in the tapping mode. Image processing and analysis was carried out with the instrument software version V612r2 and V530r2. NSG 20

DOI: 10.1021/acsnano.6b01246
ACS Nano 2016, 10, 3865−3870

cantilevers with a resonance frequency of 260 kHz and a stiffness of 28 N m^{-1} were used. AFM measurements yielded experimental parameters including the initial film thickness, the lateral distances between the generated structures, and the structures' heights and diameters.

The conductivity of the patterned film was measured by a micromanipulator (Micromanipulator Co., Serial No. 820243) with a 1 mm delicate probe and 487 PicoAmmeter/voltage source (Keithley). The electrical measurements of electrolyte gated transistors based on PPy structures in buffered aqueous media of KCl at room temperature under ambient condition were conducted by using a Keithley 2400 semiconductor source-meter and a Wonatech WBCS 3000 potentiostat.

AUTHOR INFORMATION

Corresponding Author

*E-mail: GoldberP@bham.ac.uk.

Notes

The authors declare no competing financial interest.

ACKNOWLEDGMENTS

We acknowledge funding from the EPSRC (EP/K503873/1) and the Wellcome Trust (174ISSFPP) grants. P.G.O. is a Royal Academy of Engineering Research (RAEng) Fellowship holder.

REFERENCES

(1) Katz, H. E. Chemically Sensitive Field-Effect Transistors and Chemiresistors: New Materials and Device Structures. *Electroanalysis* **2004**, *16*, 1837−1842.
(2) Wang, J. Z.; Zheng, Z. H.; Li, H. W.; Huck, W. T. S.; Sirringhaus, H. Dewetting of Conducting Polymer Inkjet Droplets on Patterned Surfaces. *Nat. Mater.* **2004**, *3*, 171−176.
(3) Katz, E.; Willner, I.; Wang, J. Electroanalytical and Bioelectroanalytical Systems Based on Metal and Semiconductor Nanoparticles. *Electroanalysis* **2004**, *16*, 19−44.
(4) Sonmez, G.; Sonmez, H. B.; Shen, C. K. F.; Wudl, F. Red, Green, and Blue Colors in Polymeric Electrochromics. *Adv. Mater.* **2004**, *16*, 1905−1908.
(5) Dong, B.; Zhong, D. Y.; Chi, L. F.; Fuchs, H. Patterning of Conducting Polymers Based on a Random Copolymer Strategy: Toward the Facile Fabrication of Nanosensors Exclusively Based on Polymers. *Adv. Mater.* **2005**, *17*, 2736−2741.
(6) Drury, C. J.; Mutsaers, C. M. J.; Hart, C. M.; Matters, M.; de Leeuw, D. M. Low-Cost All-Polymer Integrated Circuits. *Appl. Phys. Lett.* **1998**, *73*, 108−110.
(7) Parashkov, R.; Becker, E.; Riedl, T.; Johannes, H.-H.; Kowalsky, W. Microcontact Printing as a Versatile Tool for Patterning Organic Field-Effect Transistors. *Adv. Mater.* **2005**, *17*, 1523−1527.
(8) Ramanathan, K.; Bangar, M. A.; Yun, M.; Chen, W.; Mulchandani, A.; Myung, N. V. Individually Addressable Conducting Polymer Nanowires Array. *Nano Lett.* **2004**, *4*, 1237−1239.
(9) Lowe, J.; Holdcroft, S. Synthesis and Photolithography of Polymers and Copolymers Based on Poly(3-(2-(methacryloyloxy)-ethyl)thiophene). *Macromolecules* **1995**, *28*, 4608−4616.
(10) Schanze, K. S.; Bergstedt, T. S.; Hauser, B. T. Photolithographic Patterning of Electroactive Polymer Films and Electrochemically Modulated Optical Diffraction Gratings. *Adv. Mater.* **1996**, *8*, 531−534.
(11) Granlund, T.; Nyberg, T.; Roman, L. S.; Svensson, M.; Inganäs, O. Patterning of Polymer Light-Emitting Diodes with Soft Lithography. *Adv. Mater.* **2000**, *12*, 269−273.
(12) Pease, L. F., III; Russel, W. B. Charge Driven Electrohydrodynamic Patterning of Thin Films. *J. Chem. Phys.* **2006**, *125*, 184716.
(13) Pease, L. F.; Russel, W. B. Linear Stability Analysis of Thin Leaky Dielectric Films Subjected to Electric Fields. *J. Non-Newtonian Fluid Mech.* **2002**, *102*, 233−250.
(14) Pease, L. F.; Russel, W. B. Electrostatically Induced Submicron Patterning of Thin Perfect and Leaky Dielectric Films: A Generalized Linear Stability Analysis. *J. Chem. Phys.* **2003**, *118*, 3790−3803.
(15) Schaffer, E.; Thurn-Albrecht, T.; Russell, T. P.; Steiner, U. Electrically Induced Structure Formation and Pattern Transfer. *Nature* **2000**, *403*, 874−877.
(16) Mahajan, S.; Hutter, T.; Steiner, U.; Goldberg Oppenheimer, P. Tunable Microstructured Surface-Enhanced Raman Scattering Substrates *via* Electrohydrodynamic Lithography. *J. Phys. Chem. Lett.* **2013**, *4*, 4153−4159.
(17) Goldberg-Oppenheimer, P.; Steiner, U. Rapid Electrohydrodynamic Lithography Using Low-Viscosity Polymers. *Small* **2010**, *6*, 1248−1254.
(18) Goldberg Oppenheimer, P. *Electrohydrodynamic Patterning of Functional Materials*; Springer: New York, 2013.
(19) Yonngin, S. Method for Making Polypyrrole. Patent WO 02/10251, 2002.
(20) Harkema, S.; Steiner, U. Hierarchical Pattern Formation in Thin Polymer Films Using an Electric Field and Vapor Sorption. *Adv. Funct. Mater.* **2005**, *15*, 2016−2020.
(21) Morariu, M. D.; Voicu, N. E.; Schäffer, E.; Lin, Z.; Russell, T. P.; Steiner, U. Hierarchical Structure Formation and Pattern Replication Induced by an Electric Field. *Nat. Mater.* **2003**, *2*, 48−52.
(22) Harkema, S. Capillary Instabilities in Thin Polymer Films. Ph.D. Thesis, University of Groningen, 2006.
(23) Goldberg-Oppenheimer, P.; Eder, D.; Steiner, U. Carbon Nanotube Alignment *via* Electrohydrodynamic Patterning of Nanocomposites. *Adv. Funct. Mater.* **2011**, *21*, 1895−1901.
(24) Goldberg-Oppenheimer, P.; Mahajan, S.; Steiner, U. Hierarchical Electrohydrodynamic Structures for Surface-Enhanced Raman Scattering. *Adv. Mater.* **2012**, *24*, OP175−OP180.
(25) Al-Kaysi, R. O.; Ghaddar, T. H.; Guirado, G. Fabrication of One-Dimensional Organic Nanostructures Using Anodic Aluminum Oxide Templates. *J. Nanomater.* **2009**, *2009*, 1−14.
(26) Im, Y.; Vasquez, C. P.; Lee, C.; Myung, N.; Penner, R.; Yun, M. Single Metal and Conducting Polymer Nanowire Sensors for Chemical and DNA Detections. *J. Phys.: Conf. Ser.* **2006**, *38*, 61−64.
(27) Lee, M. S.; Kang, H. S.; Joo, J.; Epstein, A. J.; Lee, J. Y.; Kang, H. S. Flexible All-Polymer Field Effect Transistors with Optical Transparency Using Electrically Conducting Polymers. *Thin Solid Films* **2005**, *477*, 169−173.
(28) Alam, M. M.; Wang, J.; Guo, Y.; Lee, S. P.; Tseng, H.-R. Electrolyte-Gated Transistors Based on Conducting Polymer Nanowire Junction Arrays. *J. Phys. Chem. B* **2005**, *109*, 12777−12784.

DOI: 10.1021/acsnano.6b01246
ACS Nano 2016, 10, 3865−3870